Effect of length and rigidity of microtubules on the size of ring-shaped assemblies obtained through active self-organization

Shoki Wada,[1,#] Arif Md. Rashedul Kabir,[2,#] Masaki Ito,[1] Daisuke Inoue,[1] Kazuki Sada[1,2] and Akira Kakugo[1,2,]*

[1]Graduate School of Chemical Sciences and Engineering, Hokkaido University, Sapporo 060-0810, Japan

[2]Faculty of Science, Hokkaido University, Sapporo 060-0810, Japan

*Authors to whom correspondence should be addressed.

E-mail: kakugo@sci.hokudai.ac.jp

Telephone/fax: +81-11-706-3474

[#] These two authors contributed equally to this work.

Abstract

The microtubule (MT)-kinesin biomolecular motor system has attracted much attention due to its possible applications in artificial biomachines. Recently an active self-organization (AcSO) method has been established to integrate MT filaments into highly organized assembled structures. The ring-shaped MT assembly, one of the structures derived from the AcSO of MTs, can convert the translational motion of MTs into rotational motion. Due to this attractive feature, the ring-shaped MT assembly appears to be a promising candidate for developing artificial devices and for future nanotechnological applications. In this work, we have investigated the effect of length and rigidity of MT filaments on the size of ring-shaped MT assembly in the AcSO process. We show that the size of ring-shaped MT assembly can be controlled by tuning the length and rigidity of MT filaments employed in the AcSO. Longer and stiffer MT filaments led to larger ring-shaped assemblies through AcSO, while AcSO of shorter and less stiff MT filaments produced smaller ring-shaped assemblies. This work might be important for the development of biomolecular motor based artificial biomachines, especially where size control of ring-shaped MT assembly will play an important role.

Introduction

Biomolecular motor systems e.g. microtubule (MT)-kinesin is being used for developing artificial micro devices such as biosensor, molecular shuttle and sorting device.[1-6] For developing artificial devises *in vitro* motility assay[7] has provided the platform where kinesins are immobilized on a substrate to demonstrate sliding motion of MTs in the presence of adenosine triphosphate (ATP). Based on the expertise of the *in vitro* motility assay, recently an active self-organization (AcSO) method has been introduced as a tool for integrating MTs into highly ordered assembled structures by making use of a specific streptavidin (St)-biotin (Bt) interaction as glue among the sliding MTs.[8,9] Depending on the experimental conditions such as MT concentration and crosslinker ratio (St/Bt), AcSO of MTs provides bundle-, network-, and ring-shaped assemblies which generate translational, amoeboid and rotational motion respectively.[10,11] Among them, the ring-shaped assembly have been attracting considerable attention and appears to be a promising candidate for application in nanotechnology as this non-equilibrium structure is capable of storing a huge amount of bending energy[8] and can provide continuous work without changing the position of the mass center.[12-16] Therefore, it is important to understand how different factors affect the formation and properties of ring-shaped MT assemblies such as rotational direction, thickness (subtraction of inner diameter from outer diameter), size etc.. So far, we have successfully controlled the rotational direction[17] and thickness[18] of the ring-shaped MT assembly by tuning helical structure of MTs and by feeding MTs in a stepwise manner in the AcSO respectively. The size of ring-shaped MT assembly was reported to be tuned by changing kinesin concentration on the substrate surface[19] and also by applying space confinement in the AcSO of MTs.[20]

In this work, we demonstrate a new approach for controlling the size of ring-shaped assembly of MTs by controlling the length and rigidity of MTs in the AcSO. The length of MTs was tuned by applying shear stress[21] and the rigidity of MT was varied by polymerizing

tubulin in the presence of either guanidine triphosphate (GTP) or its analogue, Guanosine-5'-[(α,β)-methyleno]triphosphate (GMPCPP).[22] The MT prepared in the presence of GMPCPP (GMPCPP-MT) is structurally stable compared to the MT prepared in the presence of GTP (GTP-MT) and rigidity of the GMPCPP-MT is much higher than that of the GTP-MT owing to a stronger lateral interaction among protofilaments.[23] Here we report that, change in the length and rigidity of MTs in an AcSO can strongly affect the size of ring-shaped MT assembly. Increase in length and rigidity of MTs used in the AcSO increase the size (inner diameter) of the ring-shaped MT assembly, and *vice versa*. This work thus offers a protocol to prepare size-controlled ring-shaped MT assembly, which might play an important role in fostering development of biomolecular motor system based artificial biomachines in future.

Experimental section

Preparation of tubulin and kinesin

Tubulin was purified from porcine brain using a high-concentration PIPES buffer (1 M PIPES, 20 mM EGTA, and 10 mM $MgCl_2$; pH adjusted to 6.8 using KOH). The high-concentration PIPES buffer and 80 mM brain reconstitution buffer (BRB80) were prepared using PIPES from Sigma, and the pH was adjusted using KOH.[24] Recombinant conventional kinesin-1 consisting of first 573 amino acid residues of human kinesin-1 (K573) and GFP-fused kinesin-1 construct consisting of the first 560 amino acid residues of human kinesin-1 (K560) were prepared as described in previously published papers by partially modifying the expression and purification methods.[25]

Preparation of labeled tubulin

Alexa 488-labelled tubulin was prepared using Alexa Fluor 488 succinimidyl ester (Alexa Fluor 488-SE®; Invitrogen) according to the standard technique.[26] The labeling ratio of Alexa 488- modified tubulin was 1.0. This ratio was determined by measuring the absorbance of the protein and Alexa 488 at 280 nm and 495 nm respectively.

Biotin (Bt) labeling and stoichiometric estimation

Bt-labelled tubulin was prepared using biotin-XX-SE® (Invitrogen) according to the standard technique.[27] The labeling stoichiometry was approximately 0.76 per tubulin heterodimer, which was estimated by spectrometric titration using 2-(4-hydroxyphenylazo) benzoic acid (HABA) dye (Wako).[28]

Preparation of microtubule

GTP-MTs were prepared by incubating 70 μM tubulin mix (Alexa tubulin:biotin tubulin= 1:1 in molar ratio) at 37 °C for 1 hour in a polymerization buffer (80 mM PIPES, 1 mM EGTA, 5

mM $MgCl_2$, 5% DMSO, 1 mM GTP; pH~6.8). The solution containing the GTP-MTs was then diluted with motility buffer (80 mM PIPES, 1 mM EGTA, 2 mM $MgCl_2$, 0.5 mg mL^{-1} casein, 1 mM DTT, 10 μM paclitaxel and ~1% DMSO; pH~6.8). For polymerization of GMPCPP-MTs, 40 μM of tubulin mix (Alexa tubulin:biotin tubulin= 1:1 in molar ratio) was incubated at 37 °C in a polymerization buffer containing 1 mM GMPCPP (Jena Bioscience, Jena, Germany) and 5 mM $MgCl_2$. After 10 min of incubation the polymerized MTs (MT seeds) were diluted 1000-fold into an elongation buffer containing 1 μM tubulin mix, 5 mM $MgCl_2$ and 1 mM GMPCPP and incubated for 4 hours at 37 °C. The solution containing the elongated GMPCPP-MTs was then diluted with motility buffer (80 mM PIPES, 1 mM EGTA, 2 mM $MgCl_2$, 0.5 mg mL^{-1} casein, 1 mM DTT, 10 μM paclitaxel and ~1% DMSO; pH~6.8). For preparing length controlled GTP-MTs or GMPCPP-MTs, a Hamilton syringe (inner diameter: 2.06 mm) and a peek tube (nominal inner diameter: 0.26 mm) were used for the shearing treatment of MTs. 30 μL of microtubule solution in each case was passed back-and-forth (one, two, three or five times as mentioned in the discussion section) through the syringe-mounted peek tube by manual operation of a syringe.[21] Change in MT length before and after shearing treatment was manually measured using an image analysis software 'ImageJ'.

Active self-organization (AcSO) of MTs

Flow cell with dimension of 9 × 2.5 × 0.45 mm^3 (L × W × H) was assembled from two cover glasses of sizes (9 × 18) mm^2 and (40 × 50) mm^2 (MATSUNAMI) and double-sided tape was used as the spacer. First, the flow cell was filled with 5 μL of 0.1 mg mL^{-1} anti-GFP antibody (Invitrogen) or 5 μL of casein buffer (80 mM PIPES, 1 mM EGTA, 1 mM $MgCl_2$ and ~0.5 mg mL^{-1} casein; pH adjusted to 6.8). The flow cell coated with antibody was then washed with casein buffer. After incubation of both types of flow cell for 2 min, 100 nM of K560 or K573 kinesin solution (~80 mM PIPES, ~40 mM NaCl, 1 mM EGTA, 1 mM $MgCl_2$,

0.5 mg mL^{-1} casein, 1 mM DTT, 10 μM paclitaxel and ~1% DMSO; pH 6.8) was introduced into antibody coated or casein coated flow cell respectively, and the flow cells were incubated for 2 min to allow the kinesins to bind to the antibody or casein-coated glass surface. After washing the flow cell with 10 μL of motility buffer, 5 μL of 1000 nM MT solution (taxol stabilized GTP-MT, GMPCPP-MT with or without taxol as mentioned in the 'results and discussion' section) was then introduced and incubated for 2 min, followed by washing with 5 μL of motility buffer. Next, 5 μL of 100 nM streptavidin (St;Wako) solution was introduced so as to maintain the crosslinker ratio (St/Bt) at 1/3.8 in the flow cell and allowed for 2 min incubation, followed by washing with 5 μL of motility buffer. Finally, AcSO was initiated by applying 5 μL of ATP solution (motility buffer supplemented with 5 mM ATP). The time of the ATP addition was set as 0 h. The aforementioned experiments were performed at room temperature using the inert chamber system (ICS).[29] The flow cell was placed inside the inert chamber after the addition of ATP, as described in a previous report.[12] Humid nitrogen gas was continuously passed through the chamber to remove existing oxygen from the chamber. The first observation of sample (ring-shaped MT assembly) by fluorescence microscope was performed after passing the nitrogen gas for 60 min. As mentioned in the 'results and discussion' section, ~60 min was the time by which the ring-shaped MT assemblies attained a steady state.

Microscopy image capture

To observe the motility of MTs, the samples were illuminated with a 100 W mercury lamp and visualized by an epifluorescence microscope (Eclipse Ti, Nikon) using an oil-coupled Plan Apo 60×1.40 objective (Nikon). UV cut-off filter blocks (GFP-HQ: EX455-485, DM495, BA500-545; Nikon) were used in the optical path of the microscope. These blocks allowed visualization of samples but eliminated the UV part of the radiation, and minimized the harmful effect of UV radiation on the samples. Images were captured using a cooled-CMOS

camera (NEO sCMOS, Andor) connected to a PC. To capture a field of view for more than several minutes, an ND filter (ND4, 25% transmittance) was inserted into the illumination light path of the fluorescence microscope to avoid photobleaching of samples.

Image analysis

Movies of the motility assay of MTs and images captured by the fluorescence microscopy were analyzed using an image analysis software (ImageJ).

Results and discussion

The AcSO of biotinylated GTP-MTs was performed inside the inert chamber by employing the St-Bt interaction among the sliding MTs in an *in vitro* motility assay as schematically shown in Fig. 1. MT concentration was fixed at 1000 nM and the crosslinker ratio (St/Bt) was kept at 1/3.8 for allowing MTs to preferentially form ring-shaped assembly by AcSO.[10,11] Fig. S1 (see ESI) shows the time course of the AcSO and change in the number of ring-shaped MT assembly in a specific area (6.7×10^4 μm^2) over time. From this figure, it could be noticed that the number of ring-shaped MT assembly increased linearly with time and then reached a plateau (~45 min), after which no new ring-shaped assembly formation was observed. So we assumed that it took ~60 min for MTs to reach the 'steady state' in the AcSO. Here the term 'steady state' indicates the state when no new ring-shaped MT assembly was found to form and already formed ring-shaped MT assemblies were stable. This result also shows that individual ring-shaped MT assembly was formed from bundles of a few or more MTs which is in agreement with our previous observations.[18] Next GTP-MTs with different lengths were prepared by applying shear stress to MT filaments by using a micro syringe. For this, GTP-MTs were polymerized from a mixture of fluorescently labelled and biotinylated tubulins under the standard conditions mentioned in the experimental section. After polymerization, length of GTP-MTs was tuned by applying shear stress and by varying the number of shear treatment. Fig. 2 shows the change in the length and distribution of length of GTP-MTs with the change of the number of shear treatment. The distribution of length of GTP-MTs shifted to lower value and became narrower with increasing the number of shear treatment. The average length of GTP-MTs decreased from 17.3±11.7 μm (average±standard deviation) to 10.8±5.5, 5.7±3.5 and 3.7±3.0 μm after one, three and five times shear treatment respectively. Similar decrease in the average length of GTP-MTs due to shear treatment and narrowing of the distribution of MT length on decreasing the length of MTs under applied force resembles the results reported in the literature.[21,30] These length-controlled GTP-MTs

were then employed in the AcSO on a kinesin (K573) coated substrate. On addition of ATP, most of the MT filaments started to move on the kinesin coated substrate surface with a velocity of 560±20 nm s^{-1} which is comparable to that reported in a previous report.[18] Then, moving MTs started to assemble and spool to form ring-shaped MT assembly over time through the AcSO process.

Fig. 3 shows the fluorescence microsopy images of ring-shaped MT assemblies obtained from the AcSO of GTP-MTs with different average lengths. The result clearly indicates that the shorter MT filaments yielded smaller ring-shaped MT assemblies in the AcSO. When the GTP-MTs with the average length of 17.3±11.7 μm were employed, the average diameter of the ring-shaped MT assemblies was found to be 8.1±5.3 μm. However, much shorter GTP-MTs with an average length of 10.8±5.5, 5.7±3.5 and 3.7±3.0 μm provided smaller ring-shaped MT assemblies with diameter of 5.5±4.1, 3.5±2.1 and 3.0±1.4 μm respectively. Thus, the length of GTP-MTs used in the AcSO strongly affected the size of ring-shaped MT assemblies which is also evident from the Fig. S2 (see ESI), where gradual increase in size of the ring-shaped MT assemblies with increasing the length of GTP-MTs could be clearly observed. The maximum obtainable diameter of the ring-shaped MT assembly can be easily estimated from the average length of the GTP-MTs employed in the AcSO and is shown by the dotted line in Fig. S2, considering one MT filament forms a ring-shaped assembly whose circumference is equal to the length of the MT filament. One can see that the calculated diameters were slightly lower than the experimentally measured diameters in the AcSO for each of the lengths of GTP-MTs investigated. This result clearly suggests that ring-shaped MT assemblies are formed from longer bundles of MTs that are formed from the association of single MT filaments. This is also supported by *in situ* observation of ring-shaped assembly formation in our experiment (see Fig. S1 in ESI) and is in agreement with a previous report.[18] Then considering the mechanism of formation of ring-shaped MT assembly[18], that states that single MT filaments first form bundles and spooling of bundles then form ring-shaped MTs,

and assuming the similar probability of spooling it is the shorter length of GTP-MTs that seems to be the reason behind the smaller size of ring-shaped MT assembly formed in the AcSO of MTs.

Next, in order to investigate the effect of rigidity of MT filament on the size of the ring-shaped MT assembly in the AcSO, we prepared more rigid MT filaments (GMPCPP-MTs) than the GTP-MTs by polymerizing tubulin in the presence of GMPCPP instead of the GTP. To maintain similarity in experimental conditions, GMPCPP-MTs were also stabilized with taxol after preparation as was done in case of GTP-MTs (see experimental section). For employing in the AcSO, we also controlled the length of GMPCPP-MTs through shearing treatment in the similar way done for the GTP-MTs. Fig. 4 shows the fluorescence microscopy images of GMPCPP-MTs with different lengths and the distribution of their lengths at different conditions. The shearing treatment caused similar change (decrease) in length of the GMPCPP-MTs as found in case of GTP-MTs. The average length of GMPCPP-MT decreased from 10.3±5.8 μm to 7.3±3.7, 6.0±3.1 and 3.4±1.7 μm after one, three and five times shear treatment respectively. The GMPCPP-MTs with controlled lengths were then employed in the AcSO on a kinesin (K573) coated substrate. For all the lengths mentioned above, the linear GMPCPP-MT filaments were found to spool to produce ring-shaped MT assembly. As shown in the Figure 5, the diameter of the ring-shaped MT assemblies of GMPCPP-MTs decreased with decreasing the length of the GMPCPP-MTs used in the AcSO. The effect of MT length on the size of ring-shaped MT assembly observed here was similar to that observed in the case of GTP-MTs. The average diameter of the ring-shaped MT assemblies decreased from 18.8±16.9 μm to 10.0±5.0, 8.1±5.5 and 5.8±3.3 μm, when average length of GMPCPP-MTs employed in the AcSO was decreased from 10.3±5.8 μm to 7.3±3.7, 6.0±3.1 and 3.4±1.7 μm respectively. At the same time this result clearly reveals that ring-shaped assemblies obtained from the taxol stabilized GMPCPP-MTs were much larger in size than that obtained from taxol stabilized GTP-MTs. Figure 6 shows the overlay plot of the

average length of the taxol stabilized GTP-MTs and GMPCPP-MTs against the diameter of the ring-shaped assemblies they produced in respective case. The difference in size of ring-shaped MT assemblies obtained using taxol stabilized GTP- and GMPCPP-MTs can be explained qualitatively by considering the difference in rigidity between the two types of MT filaments. As the rigidty of GMPCPP-MTs (taxol stabilized) was reported to be much higher than that of taxol stabilized GTP-MTs,[31] the spooling probabilty of GMPCPP-MTs in the AcSO might be much lower than that of GTP-MTs. This is supported by the fact that GTP-MTs form bundle-shaped assemblies more easily than GMPCPP-MTs.[32] To investigate further, we performed AcSO of GMPCPP-MTs on a K573 coated substrate in the absence of taxol. Here, MTs were polymerized using GMPCPP but after polymerization the GMPCPP-MTs were not stabilized with taxol. Shearing treatment of these GMPCPP-MTs changed their length depending on the number of shear treatment as shown in the Fig. S3 (see ESI). These length controlled GMPCPP-MTs were then employed in AcSO, in the absence of taxol, to further check the dependence of size of ring-shaped MT assembly on the rigidity of MT filament. As shown in the Fig. S4, similar to the cases of taxol stabilized GTP- and GMPCPP-MTs, size of ring-shaped MT assembly decreased when the length of GMPCPP-MTs (no taxol) was decreased. Moreover the result shown in Figure 6 discloses that on elimination of taxol from the AcSO, size of ring-shaped MT assemblies obtained from GMPCPP-MTs decreased compared to that obtained from the taxol stabilized GMPCPP-MTs. This change in the size of ring-shaped MT assemblies might be correlated with the change of rigidity of GMPCPP-MT depending on the presence/absence of taxol whereas it was reported that rigidity of MTs is increased by stabilizing agents, e.g. taxol.[23] Additionally, when compared to the rigidity of taxol stabilized GTP-MTs, rigidity of GMPCPP-MTs both in the presence and absence of taxol were reported to be higher.[31] In our experiments, ring-shaped MT assemblies obtained from taxol stabilized GTP-MTs were found to be smaller in size compared to that obtained from GMPCPP-MTs both in the presence and absence of taxol.

Therefore, our results may support our hypothesis about the dependence of size of ring-shaped MT assembly on the rigidity of MT filament. Luria et. al. reported that the size of ring-shaped MT assembly changes with the root of persistence length of MT.[14] Here, by comparing the rigidity of doubly stabilized MT (taxol stabilized GMPCPP-MT) against that of taxol stabilized GTP-MT,[32] relationship between size of ring-shaped MT assembly and MT rigidity predicted by Luria et. al. could be verified. According to the report by Hawkins et. al., rigidity of doubly stabilized MT is ~4 fold higher than that of taxol stabilized GTP-MT.[31] On the other hand, since the persistence length and rigidity of MT are proportional to each other,[22] the 4 fold higher rigidity of doubly stabilized MT should result in 2 fold increase in size of ring-shaped MT assembly compared to that obtained from the taxol stabilized GTP-MT. In our work, ring-shaped MT assembly obtained from doubly stabilized MTs with an average length of 3.4±1.7 μm was found to be almost twice the size (1.9 fold larger) of that obtained from taxol stabilized GTP-MTs with an average length of 3.7±3.0 μm, which is in good agreement to that theoretically predicted by Luria et. al. (Figure 6). However when relatively longer MTs were employed in AcSO (when average length of GTP- and doubly stabilized MTs were 10.8±5.5 and 10.3±5.8 μm respectively), the prediction by Luria et. al. was found no longer valid in our work where ~3.4 times difference in size of ring-shaped MT assembly was observed which is could be observed in the Figure 6. This discrepancy suggests that for relatively longer MT filaments the rigidity of MT may not be enough to explain the change in the size of ring-shaped MT assemblies in an AcSO.

Now, length of kinesin is known to affect the movement of MTs in an *in vitro* motility assay.[33] We also investigated the effect of kinesin length on the size of ring-shaped MT assembly by varying the strucuture of tail region of kinesin. For this instead of kin573, we used kin560 in the AcSO of GTP-MTs. Kin560 might be more rigid than the Kin573 and thereby may affect the mechanical coupling with moving MT.[33] However, comparing the size of ring-shaped GTP-MT assemblies obtained on K560 and K573 coated substrate as shown in

the Fig. S2 (see ESI), we found no statistically significant difference. Therefore, it might be concluded that kinesin's mechanical coupling with moving MT has no effect in determining the size of ring-shaped MT assembly in the AcSO. Here it is to mention that, similar to the result observed using the K573 coated substrate, size of ring-shaped GTP-MT assembly also decreased on decreasing the average length of GTP-MT filaments on the K560 coated substrate, which is evident from the Fig. S5 and S6.

Finally, in this work the observed differences in the size of the ring-shaped MT assemblies in different conditions have been found to be statistically significant (see Fig. 6). This suggests that the difference in size of ring-shaped MT assemblies originated from the difference in rigidity and length of MT filaments employed in AcSO. In depth analysis of the formation process of ring-shaped MT assembly in the AcSO may help understand the role of filament length and rigidity in determining the size of ring-shaped assembly and also in MT bundle formation.

Conclusions

In conclusion, we have developed a method to control the size of ring-shaped MT assembly by varying the length and the rigidity of MT filament in the AcSO. Large ring-shaped MT assembly can be prepared through the AcSO by employing longer or rigid MT filaments. Decrease in the length or stiffness of MT filament can produce smaller ring-shaped MT assembly. Controlling the size of ring-shaped MT assembly should amplify the *in vitro* applications of the biomolecular motor system MT-kinesin and expedite the development of micro artificial biomachine in future. At the same time, understanding the factors affecting the size of ring-shaped MT assembly would allow a better approach to control the structures obtained from self-organization of MTs. Consequently this might offer means to determine non-equilibrium structures formed from active assembly process of micro or mesoscale building units in a more controlled way.[34,35]

References

1. G. L. Martin, V. D. Heuvel and C. Dekker, *Science*, 2007, **317**, 333.

2. A. Kakugo, S. Sugimoto, J. P. Gong and Y. Osada, *Adv. Mater.*, 2002, **14**, 1124.

3. S. Hiyama, R. Gojo, T. Shima, S. Takeuchi and K. Sutoh, *Nano Lett.*, 2009, **9**, 2407.

4. G. L. Martin, V. D. Heuvel, M. P. de Graaff and C. Dekker, *Science*, 2006, **312**, 910.

5. H. Hess, J. Clemmens, J. Howard and V. Vogel, *Nano Lett.*, 2002, **2**, 113.

6. H. Hess, G. D. Bachand and V. Vogel, *Chemistry-A European Journal*, 2004, **9**, 2110.

7. S. J. Kron and J. A. Spudich, *Proc. Natl. Acad. Sci. U.S.A.*, 1986, **83**, 6272.

8. H. Hess, J. Clemmens, C. Brunner, R. Doot, S. Luna, K. H. Ernst and V. Vogel, *Nano Lett.*, 2005, **5**, 629.

9. A. M. R. Kabir, A. Kakugo, J. P. Gong and Y. Osada, *Macromol. Biosci.*, 2011, **11**, 1314.

10. Y. Tamura, R. Kawamura, K. Shikinaka, A. Kakugo, Y. Osada, J. P. Gong and H. Mayama, *Soft Matter*, 2011, **7**, 5654.

11. R. Kawamura, A. Kakugo, Y. Osada, and J. P. Gong, *Nanotechnology*, 2010, **21**, 145603.

12. A. M. R. Kabir, D. Inoue, A. Kakugo, K. Sada and J. P. Gong, *Polym. J.*, 2012, **44**, 607.

13. H. Liu, E. D. Spoerke, M. Bachand, S. J. Koch, B. C. Bunker and G. D. Bachand, *Adv. Mater.* 2008, **20**, 4476.

14. I. Luria, J. Crenshaw, M. Downs, A. Agarwal, S. B. Seshadri, J. Gonzales, O. Idan, J. Kamcev, P. Katira, S. Pandey, T. Nitta, S. R. Phillpot and H. Hess, *Soft Matter*, 2011, **7**, 3108.

15. M. Ito, A. M. R. Kabir, D. Inoue, T. Torisawa, Y. Toyoshima, K. Sada and A. Kakugo, *Polym. J.*, 2014, **46**, 220.

16. O. Idan, A. T. Lam, J. Kamcev, J. Gonzales, A. Agarwal and H. Hess, *Nano Lett.*, 2012, **12**, 240.

17. A. Kakugo, A. M. R. Kabir, N. Hosoda, K. Shikinaka and J. P. Gong, *Biomacromolecules*, 2011, **12**, 3394.

18. D. Inoue, A. M. R. Kabir, H. Mayama, J. P. Gong, K. Sada and A. Kakugo, *Soft Matter*, 2013, **9**, 7061.

19. A. T. Lam, C. Curschellas, D. Krovvidi and H. Hess, *Soft Matter*, 2014**, 10**, 8731.

20. H. Liu and G. D. Bachand, *Cell. Mol. Bioeng.*, 2013, **6**, 98.

21. Y. Jeune-Smith and H. Hess, *Soft Matter*, 2010, **6**, 1778.

22. J. Howard, in *Mechanics of Motor Proteins and the Cytoskeleton*, Sinauer Associates: Sunderland, MA, 2001.

23. B. Mickey and J. Howard, *J. Cell Biol.*, 1995, **130**, 909.

24. M. Castoldi and A. V. Popov, *Protein Expression Purif.*, 2003, **32**, 83.

25. R. B. Case, D. W. Pierce, H. B. Nora, L. H. Cynthia and R. D. Vale, *Cell*, 1997, **90**, 959.

26. J. Peloquin, Y. Komarova and G. Borisy, *Nat. Methods*, 2005, **2**, 299.

27. A. Hyman, D. Drechsel, D. Kellogg, S. Salser, K. Sawin, P. Steffen, L. Wordeman and T. Mitchison, *Methods Enzymol.*, 1991, **196**, 478.

28. N. M. Green, *Methods Enzymol.*, 1970, **18**, 418.

29. A. M. R. Kabir, D. Inoue, A. Kakugo, A. Kamei and J. P. Gong, *Langmuir*, 2011, **27**, 13659.

30. A. M. R. Kabir, D. Inoue, Y. Hamano, H. Mayama, K. Sada and A. Kakugo, *Biomacromolecules*, 2014, **15**, 1797.

31. T. L. Hawkins, D. Sept, B. Mogessie, A. Straube and J. L. Ross, *Biophysical J.*, 2013, **104**, 1517.

32. R. Kawamura, A. Kakugo, Y. Osada and J. P. Gong, *Langmuir*, 2009, **26**, 533.

33. P. Bieling, I. A. Telley, J. Pichler and T. Surrey, *EMBO reports*, 2008, **9**, 1121.

34. G. M. Whitesides and B. Grzybowski, *Science*, 2002, **295**, 2418.

35. M. Fialkowski, K. J. M. Bishop, R. Klajn, S. K. Smoukov, C. J. Campbell and B. A. Grzybowski, *J. Phys. Chem. B*, 2006, **110**, 2482.

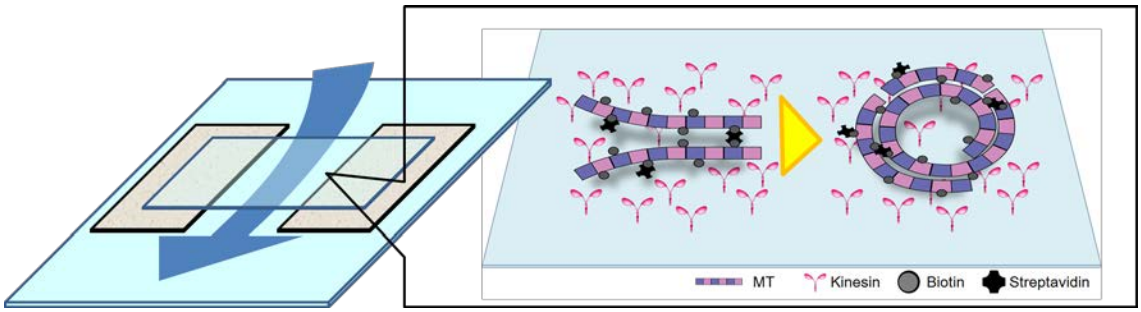

Fig. 1: Schematic representation of the active self-organization (AcSO) of MTs performed in a glass flow cell. A specific streptavidin (St)-biotin (Bt) interaction was employed for the AcSO of MTs sliding on a kinesin-coated surface that resulted in ring-shaped MT assembly.

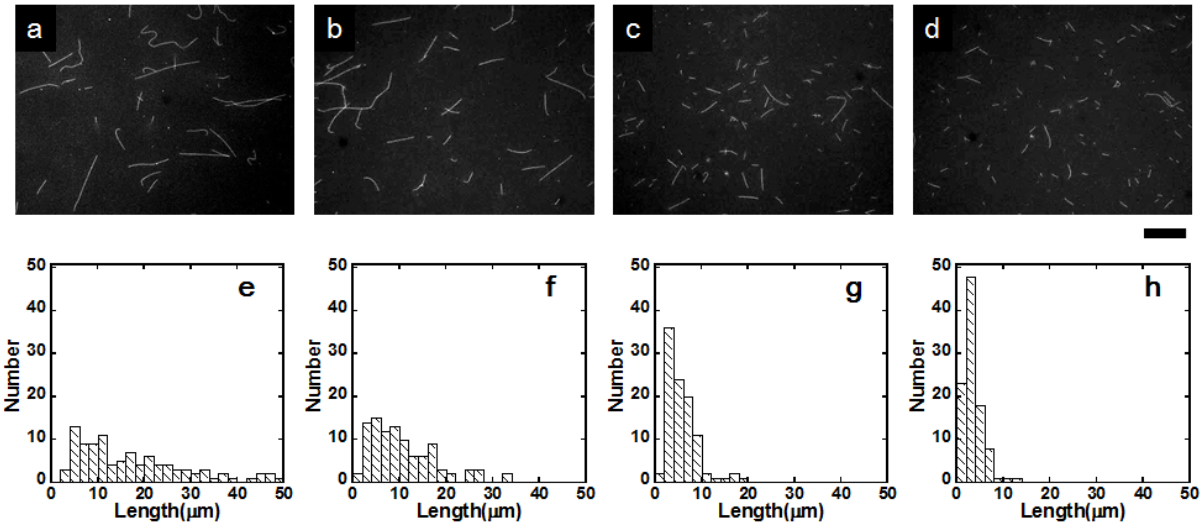

Fig. 2: Fluorescence microscopy images of GTP-MTs: (a) before and (b-d) after shear treatment. For shearing, MT solution was passed back-and-forth (b) one, (c) three and (d) five times through a syringe-mounted needle by manual operation of the syringe. Histograms show the distribution of GTP-MT length at different conditions: (e) no shearing and shearing treatment for (f) one, (g) three and (h) five times. The average length of GTP-MT decreased from (e) 17.3±11.7 μm to (f) 10.8±5.5, (g) 5.7±3.5 and (h) 3.7±3.0 μm after one, three and five times shear treatment respectively. Number of MT considered for analyses was 100 in each case. Scale bar: 20 μm.

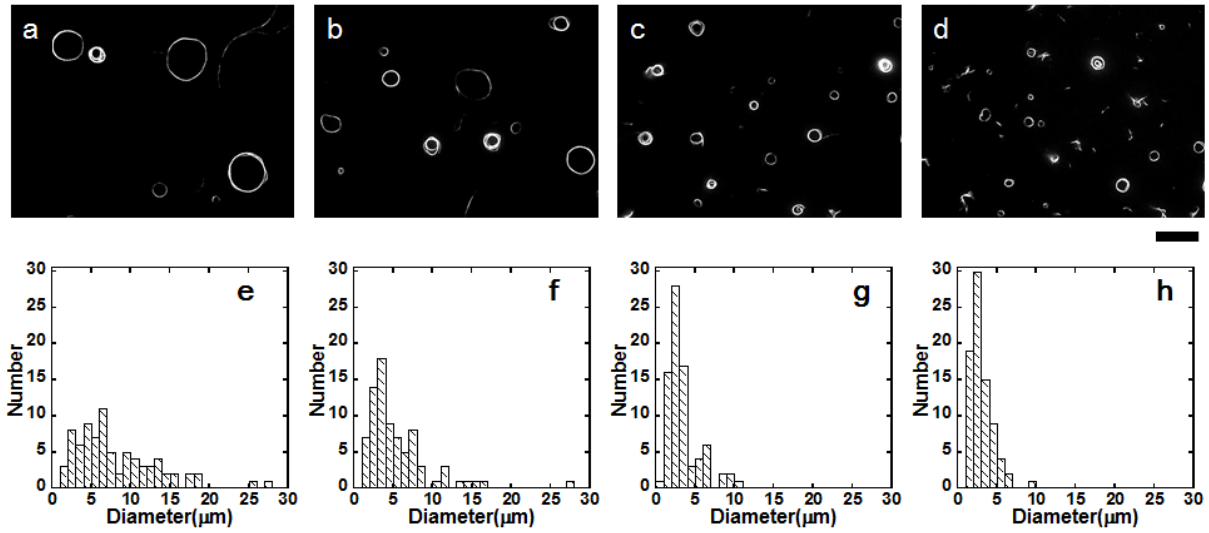

Fig. 3: Fluorescence microscopy images (a-d) of ring-shaped assemblies obtained from the AcSO of GTP-MTs with different lengths shown in the Figure 2 (a-d). As seen from these images and also from the histograms of size distribution of ring-shaped MT assemblies (e-h), with the decrease of MT length due to shearing treatment, the size (inner diameter) of ring-shaped MT assemblies also decreased. Histograms were prepared by analyzing the inner diameter of ring-shaped assemblies obtained from the AcSO of GTP-MTs that underwent: (e) no shearing and shearing treatment for (f) one, (g) three and (h) five times before being employed in the AcSO. The average diameter of ring-shaped MT assemblies decreased from (e) 8.1±5.3 μm to (f) 5.5±4.1, (g) 3.5±2.1 and (h) 3.0±1.4 μm due to one, three and five times shear treatment of MT filaments respectively. Scale bar: 20 μm.

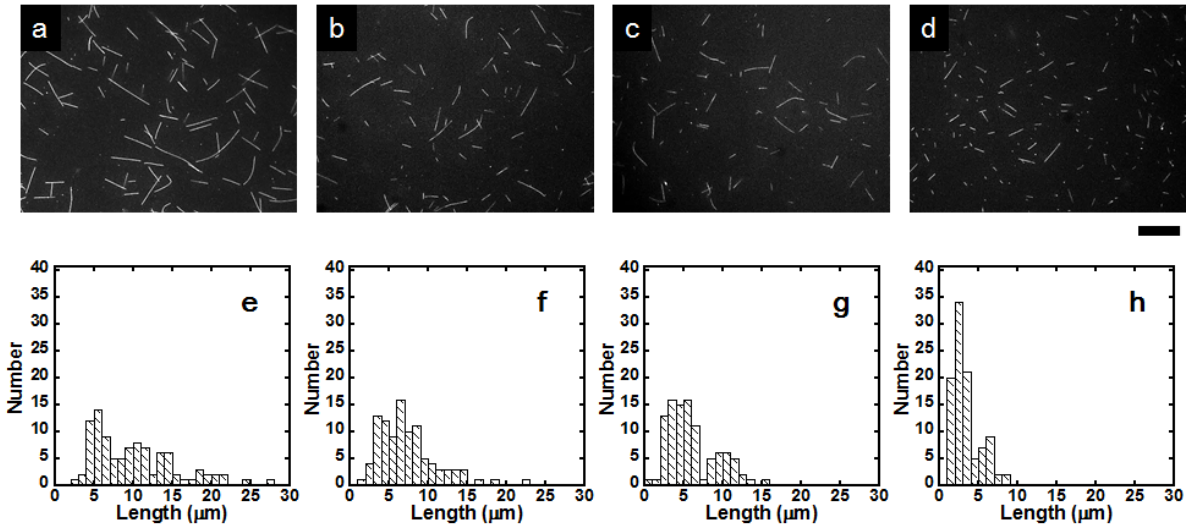

Fig. 4: Fluorescence microscopy images of taxol stabilized GMPCPP-MTs: (a) before and (b-d) after shear treatment. For shearing, MT solution was passed back-and-forth (b) one, (c) three and (d) five times. Histograms show the distribution of GMPCPP-MTs length at different conditions: (e) no shearing, shearing treatment for (f) one, (g) three and (h) five times. The average length of GMPCPP-MTs decreased from 10.3±5.8 μm to 7.3±3.7, 6.0±3.1 and 3.4±1.7 μm after one, three and five times shear treatment respectively. Number of MTs considered for analyses was 100 in each case. Scale bar: 20 μm.

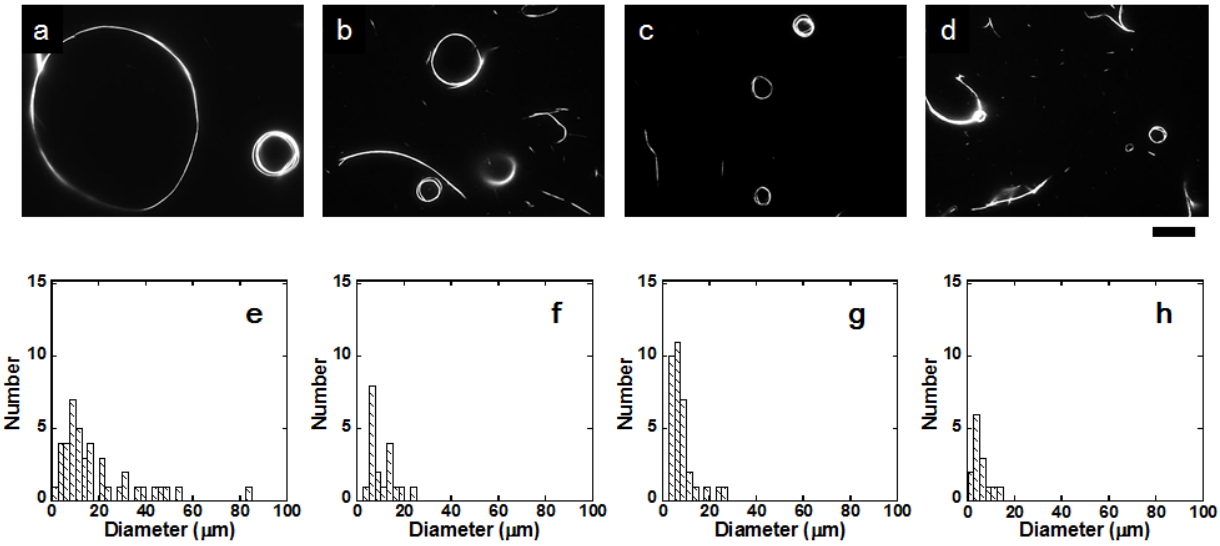

Fig. 5: Fluorescence microscopy images of ring-shaped assemblies obtained from the AcSO of taxol stabilized GMPCPP-MTs with different lengths shown in the Fig. 4 (a-d). As seen from these images and also from the histograms of size distribution of ring-shaped MT assemblies (e-h), with the decrease of MT length due to shearing the size (inner diameter) of ring-shaped assemblies also decreased. Histograms were prepared by analyzing the inner diameter of ring-shaped assemblies obtained from the AcSO of taxol stabilized GMPCPP-MTs that underwent: (e) no shearing, (f) one, (g) three and (h) five times shearing treatment before being employed in the AcSO. The average diameter of the ring-shaped MT assemblies decreased from 18.8±16.9 μm to 10.0±5.0, 8.1±5.5 and 5.8±3.3 μm after one, three, and five times shear treatment of MT filaments respectively. Scale bar: 20 μm.

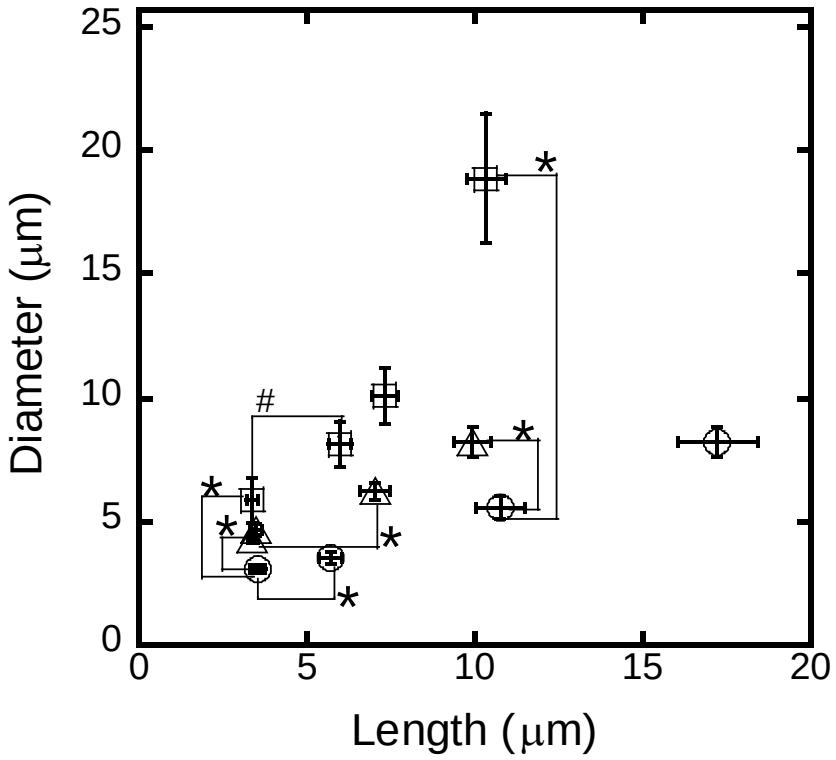

Fig. 6: Average diameter of ring-shaped MT assemblies obtained from the AcSO of length controlled taxol stabilized GMPCPP-MTs (square), GMPCPP-MTs (triangle) and taxol stabilized GTP-MTs (circle) on K573 coated substrate. The difference in size of ring-shaped MT assemblies due to change in length and rigidity of MTs in AcSO was found to be statistically significant (*$P<0.01$, $^{\#}P<0.05$ using student's t-test). Error bar: standard error of mean.

Table of contents entry

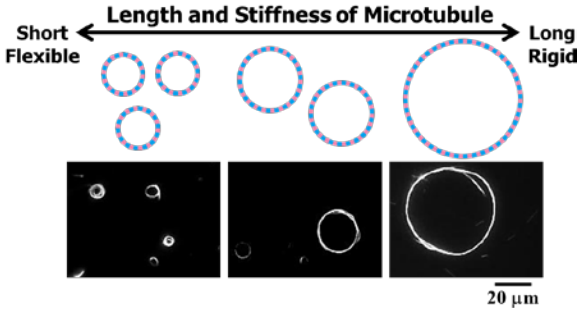

Length and stiffness of microtubule play important roles in determining the size of ring-shaped assembly in an active self-organization process.

Electronic Supplementary Information (ESI)

Effect of length and rigidity of microtubules on the size of ring-shaped assemblies obtained through active self-organization

Shoki Wada,[1,#] Arif Md. Rashedul Kabir,[2,#] Masaki Ito,[1] Daisuke Inoue,[1] Kazuki Sada,[1,2] and Akira Kakugo[1,2,]*

[1]Graduate School of Chemical Sciences and Engineering, Hokkaido University, Sapporo 060-0810, Japan

[2]Faculty of Science, Hokkaido University, Sapporo 060-0810, Japan

*Authors to whom correspondence should be addressed.

E-mail: kakugo@sci.hokudai.ac.jp

Telephone/fax: +81-11-706-3474

[#] These two authors contributed equally to this work.

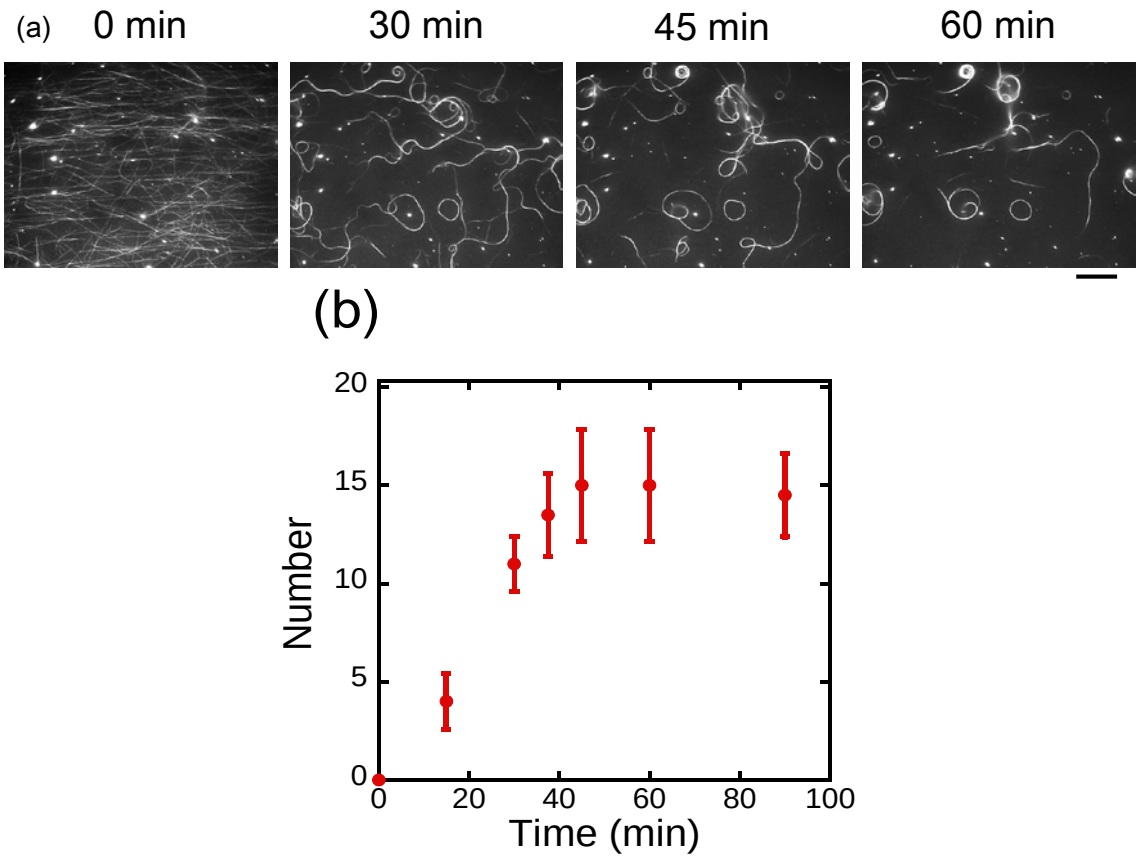

Fig. S1: (a) Fluorescence microscopy images showing the time course of AcSO of GTP-MTs that finally formed stable ring-shaped MT assemblies by ~45 min. (b) The change in the number of ring-shaped MT assemblies with time in a specific area when GTP-MTs were employed in the AcSO. Error bar: standar deviation and scale bar: 20 μm.

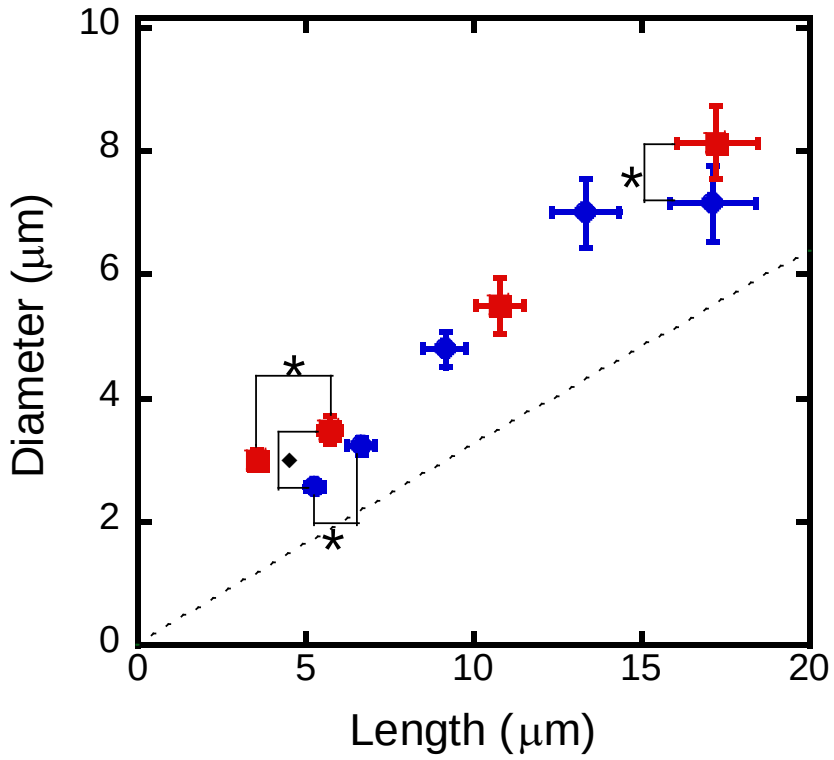

Fig. S2: Average diameter of ring-shaped MT assemblies obtained from the AcSO of length tuned GTP-MTs on substrates coated with K560 (blue circle) and K573 (red square). Dotted line represents the theoretically calculated diameter obtained from corresponding average MT length considering one MT filament forms a ring-shaped assembly whose circumference is equal to the length of the MT filament. From the statistical analyses (student's t-test), the differences in size of ring-shaped MT assemblies due to change in the length of MTs employed in the AcSO were found to be statistically significant (*$P<0.01$). The difference in size of ring-shaped MT assemblies due to change in the length of kinesin in the AcSO were not statistically significant (◆ $P>0.05$), although for longer MTs the difference was considerable (*$P<0.01$). Error bar: standard error of mean.

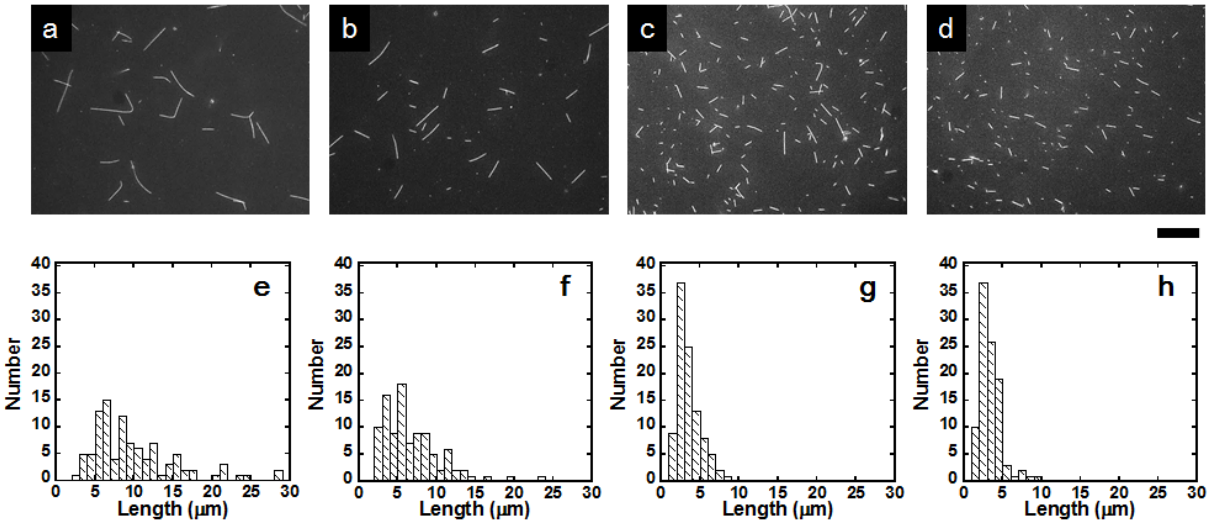

Fig. S3: Fluorescence microscopy images of GMPCPP-MTs (in the absence of taxol): (a) before and (b-d) after shear treatment. For shearing MT solution was passed back-and-forth (b) one, (c) three and (d) five times through a syringe-mounted needle by manual operation of the syringe. Histograms show the distribution of GMPCPP-MTs length at different conditions: (e) no shearing, shearing treatment for (f) one, (g) three and (h) five times. The average length of MTs decreased from 10.0±5.5 μm to 7.1±4.5, 3.5±1.5 and 3.4±1.4 μm after one, three and five times shear treatment respectively. Number of MTs considered for analyses was 100 in each case. Scale bar: 20 μm.

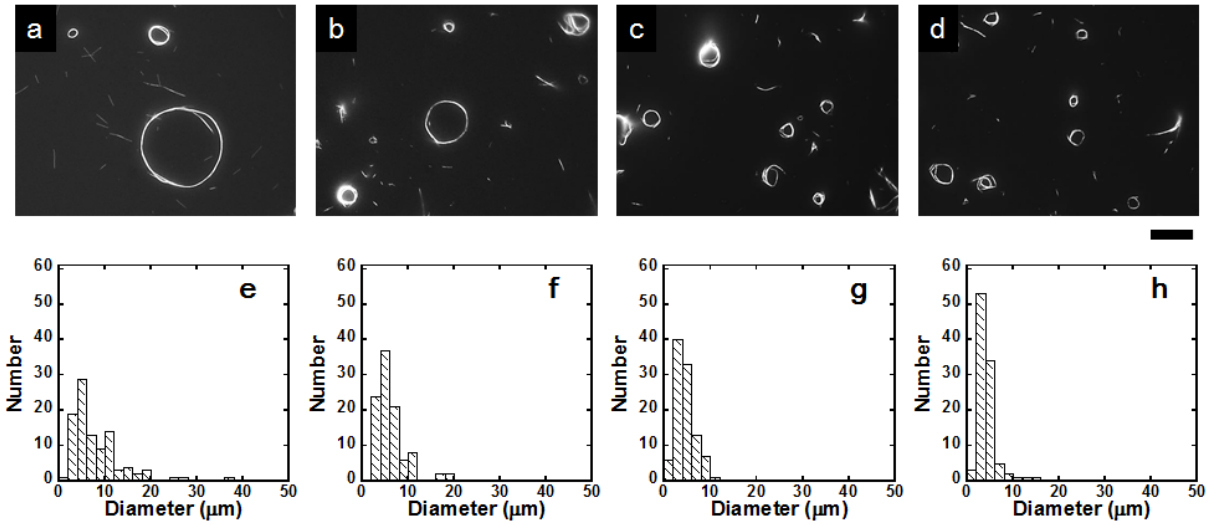

Fig. S4: Fluorescence microscopy images of ring-shaped assemblies on the K573 coated substrate obtained from the AcSO of GMPCPP-MTs (in the absence of taxol) with different lengths shown in the Fig. S3 (a-d). As seen from these images and also from the histograms of size distribution of ring-shaped MT assemblies (e-h), with the decrease of MT length due to shearing, size (inner diameter) of ring-shaped MT assemblies decreased. Histograms were prepared by analyzing the inner diameter of ring-shaped assemblies obtained from the AcSO of GMPCPP-MTs (no taxol) that underwent: (e) no shearing, (f) one, (g) three and (h) five times shearing before being employed in the AcSO. The average diameter decreased from 8.2±5.7 μm to 6.2±3.4, 4.6±2.1 and 4.3±2.1 μm after one, two, three and five times shear treatment of MT filaments respectively. Scale bar: 20 μm.

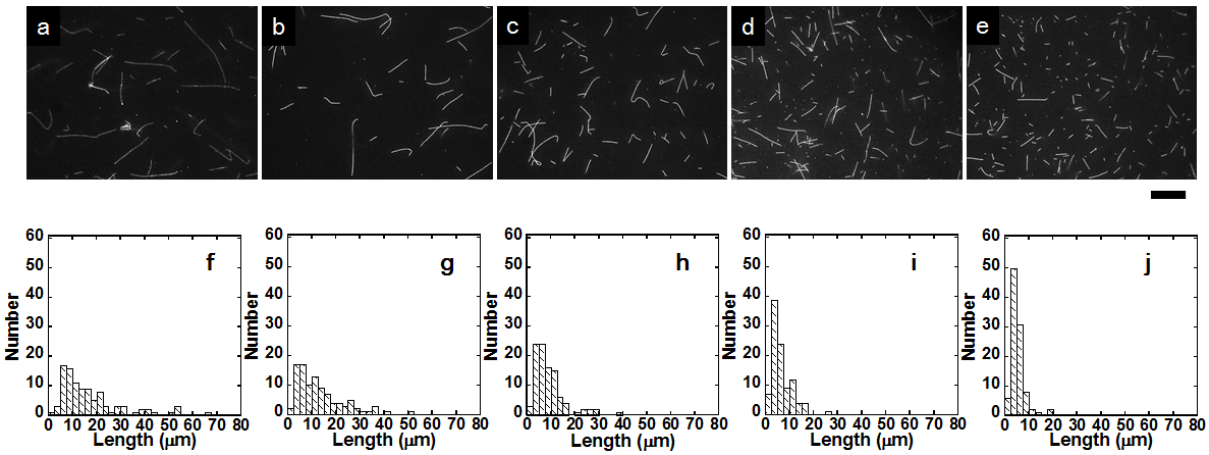

Fig. S5: Fluorescence microscopy images of GTP-MTs: (a) before and (b-e) after shear treatment. For shearing treatment, MT solution was passed back-and-forth (b) one, (c) two, (d) three and (e) five times through a syringe-mounted needle by manual operation of the syringe. Histograms show the distribution of GTP-MT length at different conditions: (f) no shearing, shearing treatment for (g) one, (h) two, (i) three and (j) five times. The average length of GTP-MT decreased from (f) 17.1±12.8 μm to (g) 13.4±9.9, (h) 9.2±6.4, (i) 6.7±4.2 and (j) 5.3±2.9 μm after one, two, three and five times shear treatment respectively. Number of MT considered for analyses was 100 in each case. Scale bar: 20 μm.

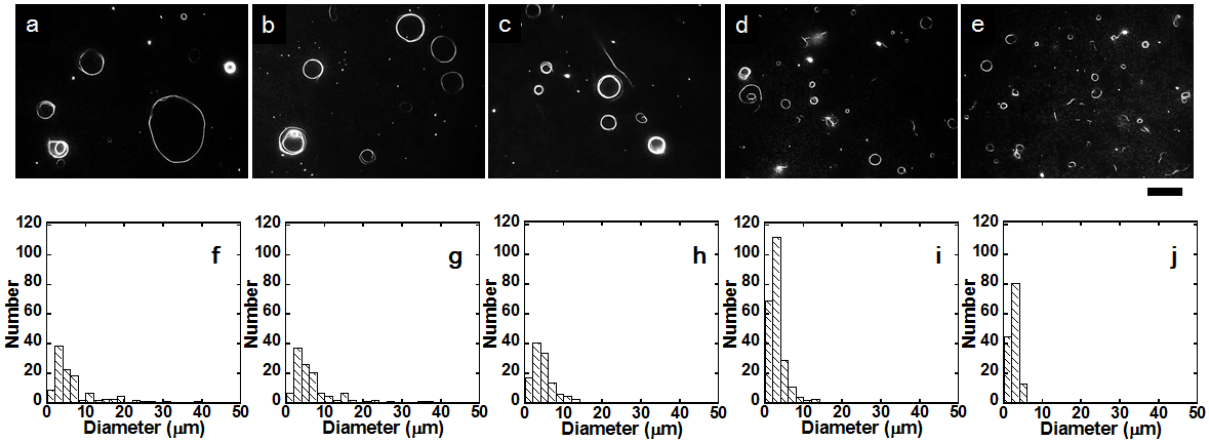

Fig. S6: Fluorescence microscopy images (a-e) of ring-shaped assemblies obtained from the AcSO of GTP-MTs with different lengths shown in the Fig. S5 (a-e). The AcSOs were performed on the K560 coated substrate. As seen from these images and also from the histograms of size distribution of ring-shaped MT assemblies (f-j), with the decrease of MT length due to shearing treatment the size (inner diameter) of ring-shaped MT assemblies also decreased. Histograms were prepared by analyzing the inner diameter of ring-shaped assemblies obtained from the AcSO of GTP-MTs that underwent: (f) no shearing, (g) one, (h) two, (i) three and (j) five times shearing before being employed in the AcSO. The average diameter of ring-shaped MT assemblies decreased from (f) 7.2±6.7 μm to (g) 7.0±6.1, (h) 4.8±3.3, (i) 3.2±2.1 and (j) 2.6±1.1 μm due to one, two, three and five times shear treatment of MT filaments respectively. Scale bar: 20 μm.